Environ. Sci. Technol. 2003, 37, 5116–5126

Transport Dynamics in a Sheltered Estuary and Connecting Tidal Straits: SF_6 Tracer Study in New York Harbor

THEODORE CAPLOW,*,† PETER SCHLOSSER,†,‡,§ DAVID T. HO,†,§ AND NICHOLAS SANTELLA†,§

Department of Earth and Environmental Engineering, Columbia University, New York, New York 10027, Lamont–Doherty Earth Observatory of Columbia University, Palisades, New York 10964, and Department of Earth and Environmental Sciences, Columbia University, New York, New York 10027

In July 2002, ~0.9 mol of sulfur hexafluoride (SF_6) was injected into Newark Bay, NJ, a 14 km^2 estuary that forms part of New York Harbor, to investigate circulation, mixing, and the transport and fate of solutes. The SF_6 tracer was observed over 11 consecutive days using a high-resolution measurement system. Total tracer mass in the sheltered waters declined quasiexponentially at a rate of 0.29 ± 0.03 d^{-1}. Air–water gas exchange was estimated to account for 56% of tracer mass loss, upon the basis of wind speed/gas exchange parametrizations. Large-scale tidal transfer of solutes through the Kill van Kull strait (7 km long) caused net seaward flushing contrary to the apparent residual circulation. Seaward transport via the Arthur Kill strait (20 km long) appeared to depend on longitudinal dispersion, residual circulation, and freshwater discharge and was ~1 order of magnitude lower. The loss rate due to flushing alone was 0.13 ± 0.02 d^{-1}, indicating a mean residence time for water and solutes in Newark Bay of ~8 days (without gas exchange). The experiment provides direct visualization of the transport of a released contaminant, and suggests a relationship between the length and configuration of tidal straits and related transport of solutes.

Introduction

The mixing and transport of contaminants in the waterways of a large urban harbor has many management implications from both environmental and economic perspectives. The pathways taken by accidental or deliberate discharges of pollutants through both dissolved and sediment phases determine their spatial and temporal distribution. In enclosed waters, contaminant concentrations tend to be higher than in open areas, and the residence time of these waters is an important determinant of consequent damage to the biota. Another area of interest is the partitioning of discharges among multiple different seaward pathways, where such pathways are available. In a harbor subject to navigational dredging, these investigations are sometimes motivated by the need for clean and efficient clearing of ship channels while minimizing resuspension of contaminated sediments and redeposition in previously dredged areas.

Although the mechanics of sediment deposition and suspension are complex, significant insights into the behavior of both suspended and dissolved contaminants can be gained by applied studies of flow and mixing. Traditional techniques used for such studies in the port areas of New York Harbor include moored current profilers (*1*) and numerical models (*2, 3*). The former method is limited by low spatial resolution, whereas the latter offers limited mixing information unless validated by empirical data specifically tailored to observe mixing. Deliberate releases of sulfur hexafluoride (SF_6) offer an alternative or complementary methodology for circulation and mixing studies. SF_6 is chemically stable, nontoxic, and has an extremely low detection limit (via gas chromatography), all factors that contribute to its successful use as a deliberate tracer in lakes, rivers, estuaries, coastal areas, and the open ocean (e.g., *4, 5, 6, 7, 8*). Used as a tracer, SF_6 is analogous to fluorescent dyes such as Rhodamine WT, but the mass of SF_6 required to achieve comparable temporal and spatial coverage is several orders of magnitude smaller. SF_6 is stable in the environment, with gas exchange across the air–water interface as the only major loss term from aquatic systems over time scales of weeks or months. As a result, mass inventories can be used to estimate the gas transfer velocity (e.g. *6, 7, 8, 9*).

Study Location. Officially recognized as the Port of New York and New Jersey, the complex of maritime facilities surrounding New York Harbor (Figure 1) is the third busiest port in the United States. Approximately 100 million tons (worth $82 billion) of dry cargo and 5000 ship arrivals per year (*10*) generate $29 billion in local trade and nearly 170 000 jobs (*11*). The areas north and west of Staten Island contain the majority of the shipping terminals. This region (collectively referred to herein as the "inner waterways") includes Newark Bay (NB; 14 km^2), the Kill van Kull (KVK; 5 km^2), and the Arthur Kill (AK; 18 km^2). The Hudson River, Raritan River, Hackensack River, and Passaic River drain a collective watershed of 42 200 km^2 into the harbor area. The latter two rivers drain 3000 km^2 directly into NB. The inner waterways generally manifest the highest levels of water and sediment contamination in the greater Hudson River estuary; prominent pollutants include PCB's, dioxins, PAHs, and heavy metals (*12, 13, 14*).

Before the construction of the port, this area was characterized by salt marshes and wide, shallow estuaries. Today, dredged ship channels begin near Ambrose Light, some 35 km seaward of NB, and extend throughout the inner waterways. A dredging project with a completion date of 2003 will deepen central NB and the KVK to 13.7 m (45 ft) from the current control depth of 12.2 m (40 ft), and plans (completion date: 2009) call for a further deepening of this entire system, including the northern end of AK, to 15.2 m (50 ft). Dredging is conducted by clamshell and dipper dredge, with large amounts of contaminated spoil typically allocated between an offshore dumpsite, underwater disposal pits in NB, and landfill caps (*15*). In an effort to minimize dredging costs, the state of New Jersey is engaged in a multiyear study to determine the sources and fates of sediments and contaminants throughout the inner waterways. The dredged channels contain more than one-half of the entire volume of the inner waterways, so their enlargement may have an impact on the transport mechanisms investigated in this

* Corresponding author phone: (212)854-0640; fax: (212)854-7081; e-mail: tc144@columbia.edu.
† Department of Earth and Environmental Engineering.
‡ Lamont–Doherty Earth Observatory.
§ Department of Earth and Environmental Sciences.

10.1021/es034198+ CCC: $25.00 © 2003 American Chemical Society
Published on Web 10/22/2003

Newark Bay Study Area
NBSA-00020

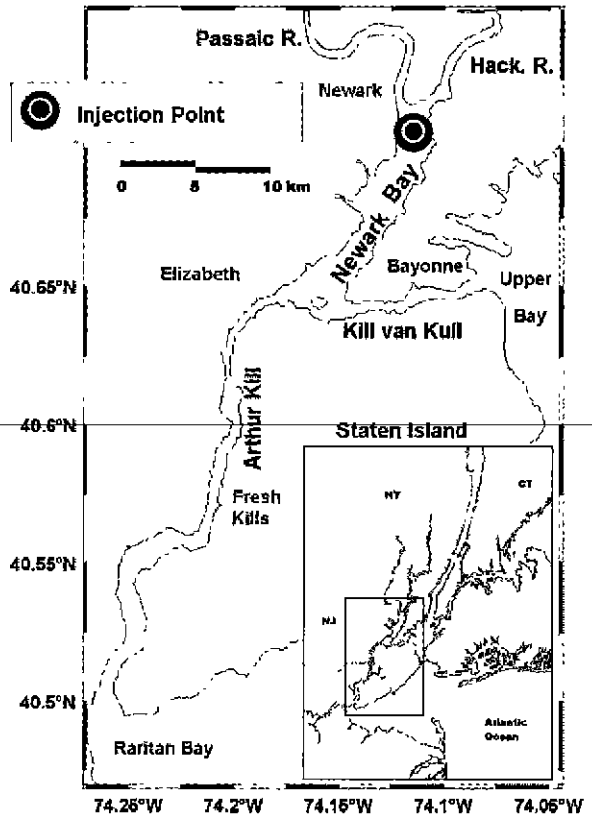

FIGURE 1. Overview of New York Harbor, showing SF_6 injection location.

study, although the nature of this impact is as yet undetermined.

Estuarine Structure and Residual (Subtidal) Circulation. More than one-half of the water in the inner waterways is oceanic in origin, with salinity exceeding 20 throughout the study area during dry (low flow) conditions. Complex tidal phase differences between the two kills, each representing a separate pathway to the sea from NB, make prediction of currents problematic. Blumberg et al. (*2*) present a model of the greater New York Harbor system with validation data from selected monitoring stations, but coverage of the inner waterways is sparse. The model predicts an estuarine flow pattern (net inland flow at bottom; net seaward flow at surface) in the inner waterways, with counterclockwise residual circulation around Staten Island, defined as a net flow westward through the KVK, and a larger net flow, augmented by river discharge, southward through the AK. On the basis of data acquired over a 301-day period in 1997–1998 from a moored acoustic Doppler current profiler (ADCP) at the western end of the KVK, Chant (*1*) suggests that stratification is enhanced and mixing is suppressed during high river discharge periods, and that the opposite is true during dry periods. The ADCP data also show a mean, depth-averaged, center-channel, inland (counterclockwise) flow of 3 cm s^{-1} during periods of low river discharge. A detailed, hourly 3-D model of the inner waterways is in late-stage development at NOAA's Office of Coast Survey (OCS) (*3*). Model runs, constrained by tides and hydrologic data for the study period, were performed at NOAA, and the output was verified using a single NOAA-maintained ADCP installed in NB near the mouth of the KVK. (This unit replaced the ADCP in the KVK at some time prior to July 2002). Model results from a full cross section of the KVK (~2 km east of NB) were provided by Wei (*16*). They indicate a net inland (counterclockwise) residual flow (with 1 cm s^{-1} typical velocity) during days 0 through 6 of the study period (day 0 was July 14, 2002), and a slower, net seaward (clockwise) residual flow for the remaining days (Figure 2). These model results must be treated as preliminary and approximate, because the model was designed for the prediction of tidal current velocities and water levels rather than for the isolation of the subtidal circulation.

Freshwater Flow. Freshwater flow during the experiment was light, punctuated by a precipitation-induced higher flow event on days 6–8 (Figure 2). For the Passaic River, the average recorded flow (4.2 m^3 s^{-1}) for July 2002 was in the 8th percentile over the 104-y record period, and the 6th percentile over the last 20 y. Limiting the comparison to July records only, the 2002 flow was in the 15th percentile over 104 y and the 10th percentile over 20 y. Hackensack River flow data were not available for the study period, but analysis of historical data from 1996 to 2001 indicates that, on average, the flow is 7% of that in the Passaic River

Tides. Data from a USGS tidal gauge on the Passaic River at Newark, NJ indicate that the M2 + S2 cycle produced spring tides on July 10 (new moon) and July 24 (full moon), with an intervening neap tide on July 17. The mean tidal range during the study period (July 14–25) was 1.97 m, which is within 9% of the summer 2002 mean for this location (1.83 m). The minimum and maximum tidal ranges during the study period were 1.86 m (neap tide) and 2.25 m (spring tide), respectively. The tracer method described here was not precise enough to differentiate solute transport across this modest span, but tidal data from the entire summer of 2002 indicate that the increase from neap tide to spring tide can be as much as 70%. If the release of a solute into Newark Bay were to occur at either the extreme neap or extreme spring tides, the flushing behavior could be significantly faster or slower than that observed here.

Methods

An automated, high-resolution, SF_6 measurement system (*7*) was used during the experiment. The system includes a pump submerged at a depth of 1.2 m, a flow-through membrane contactor to extract gases from the water, and a gas chromatograph equipped with an electron capture detector (GC-ECD). A continuous measurement interval of 2 min was achieved. Vertical profiles of salinity (conductivity) and temperature were taken at selected stations on a daily basis using manual deployment of a CTD (Seabird SBE 19plus). In addition, two complete longitudinal CTD sections (with center-channel stations spaced at 0.9 km) were made of all parts of the inner waterways during the study period.

Tracer Injection. On July 14, 2002, ~2.4 mol of SF_6 was bubbled through a coil of perforated hose (7 m long, 0.6-cm i.d., 150-μm pores) that was wrapped around a weight and towed twice across the navigable channel at a depth of 7 m at the north end of NB (Figure 1). The technique applied in this experiment was identical to that used in two prior tracer release experiments on the Hudson River (*7, 8*). Subsequent mass inventory estimates show that ~0.94 ± 0.18 mol of SF_6 (~39%) dissolved into the water column.

Sampling Strategy. The SF_6 patch was tracked for 11 consecutive days (day 1 to day 11; the injection day is designated as day 0). Horizontal transects were completed almost exclusively down the center of the dredged channel, with a sampling depth of 1.2 m and a typical spacing of 400 m. A total of 31 vertical SF_6 profiles were taken, more or less equally distributed in time throughout the experiment, typically with duplicate samples from each of three or four evenly spaced depths between the surface and the bottom. The lower 7 km of the Hackensack River was also sampled extensively on a nearly daily basis. Three sections were extended to a point 15 km upriver, on days 4, 8, and 11. The neighboring Passaic River was also sampled, although less

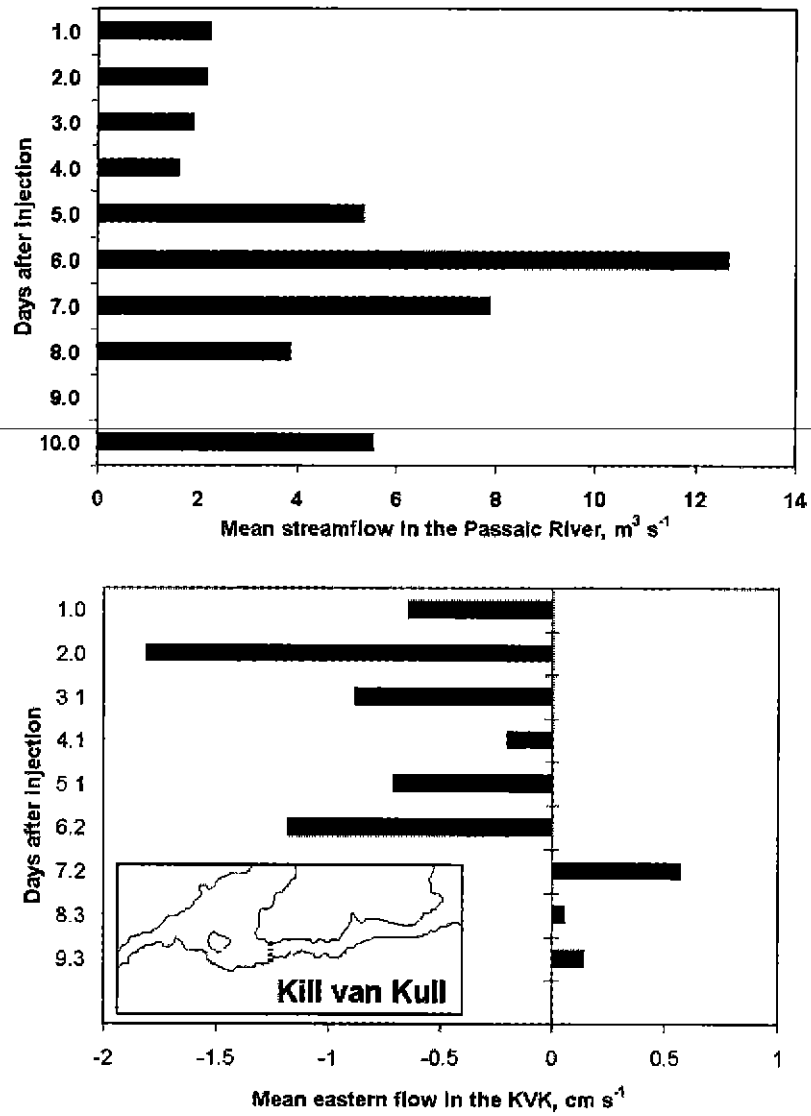

FIGURE 2. Measured streamflow in the Passaic River (at Little Falls, NJ) from a NOAA gauge (top) and modeled mean flow velocity in the KVK (location shown on map) from a preliminary NOAA modeling program (bottom). Model flows were averaged over two successive tidal cycles to remove bias stemming from the offset between 24-hour days and tidal cycles. The NOAA model indicates prevailing westward flow in the KVK until a high precipitation event on days 5 and 6. The tidal transport of SF_6e astward through the KVK was not significantly impacted by variance in the residual flow (see text; Figures 7 and 9). Note: on day 9, there was no data from the Passaic gauge.

frequently, with one significant sampling campaign on day 8 to a point 17 km upriver. The waters of Raritan Bay and the Verrazano Narrows, representing the seaward connection between the AK and the KVK, were sampled on days 4 and 10. Finally, the Hudson River was sampled as far north as the George Washington Bridge (18 km upstream) on days 6 and 12.

Complex geometry and tidal patterns in the inner waterways make synchronization of the data via tidal correction problematic. Accordingly, measured SF_6 concentrations are presented on a daily time scale without addressing tidal state or intraday sampling sequence. As a consequence, comparisons between any 2 or 3 adjacent days should be viewed with caution; it is preferable to consider as much of the full 11-day time-series as possible when interpreting the results. Data visualization software (Ocean Data View) was used to apply a 2-D grid to the study domain. Average concentrations were determined for each cell in the grid, and the resulting surface was plotted for each day. Each cell may contain data from separate transects taken at different times during the day. Typically, one or two transects were completed per day, except on day 1, when several additional transects were made.

Results

Salinity Structure. CTD surveys (Figure 3) indicate an estuarine structure throughout the study area, with salinity generally increasing with depth. Salinity throughout the inner waterways ranged from ~20 to 30 over the study period, with typical surface-to-bottom gradients of 1 to 2. A few areas appear more vertically homogeneous, including areas in the AK (around 12 km; Figure 3a) and the KVK (around 5 km; Figure 3a), as well as in the northern end of NB. These changes in vertical structure along the length of the kills appear to indicate tidal mixing. In addition, the intrusion of denser water from the KVK into the AK−NB transect can be seen in the data (at 23 km; Figure 3a). This patch of dense water is explained by the shorter length of the KVK (7 km) in

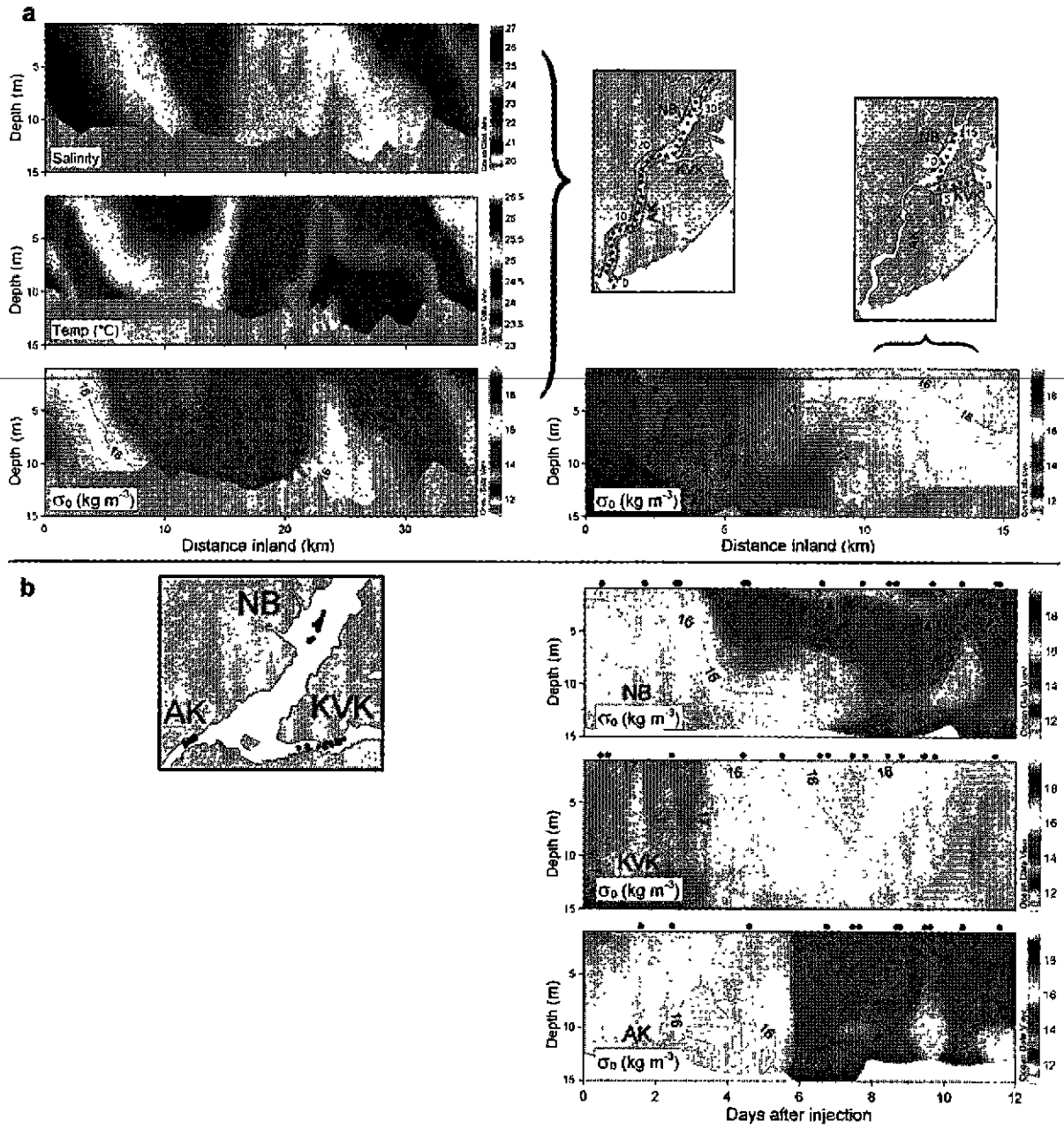

FIGURE 3. (a) Longitudinal CTD transects (station indexes shown on maps). At left, salinity, temperature, and computed potential density (σ_0) in AK and NB (from day 7); at right, σ_0 in KVK and NB (from day 0). (b) CTD time-series of σ_0 from three locations, AK, KVK, and NB (sample times are shown by dots above the graphs; dots in the map show sample locations).

comparison with the AK (20 km), because the tide brings well-mixed water from the Upper Bay quite far inland though the KVK during a single tidal cycle. Time-series of potential density indicate a slight freshening of the study area as a result of increased river flow, as previously noted, on days 6–8 (Figure 3b). Peak tidal surface velocities (determined from repeated field observations at center-channel of boat drift via GPS) of approximately 1.0 m s^{-1} in the KVK and approximately 0.55 m s^{-1} in the AK suggest net surface tidal excursions of ~14 km and ~8 km, respectively, if a sinusoidal velocity distribution is assumed. Model results (NOAA OCS) indicate a vertically averaged tidal excursion in the KVK during the study period ranging from 11.4 to 16.3 km d^{-1}, with a mean of 13.4 km d^{-1}.

SF_6 Distribution. Daily surface SF_6 distributions for 11 consecutive days illustrate the general transport and mixing properties of the inner waterways (Figure 4). Maximum SF_6 concentrations on days 1, 6, and 11 were ~8600, ~1000, and ~150 fmol L^{-1}, respectively. SF_6 spread within 1 day through NB, the KVK, and up into the Hackensack and Passaic rivers. Transport into and through the AK was much slower. After 11 days, large-scale tidal mixing and air–water gas exchange had removed most of the SF_6 from the inner waterways. Measurements taken just outside the AK and the KVK (Figure 5) indicate that for the first 6 days following injection, nearly all of the net flushing was via the KVK. In the second week, the SF_6 signal was detected in Raritan Bay at the mouth of the AK. By day 10, the channels contained roughly equal concentrations of SF_6.

Although the initial vertical distribution of SF_6 resulting from the injection process is not known, daily vertical SF_6 profiles, beginning the day after injection, indicate that at

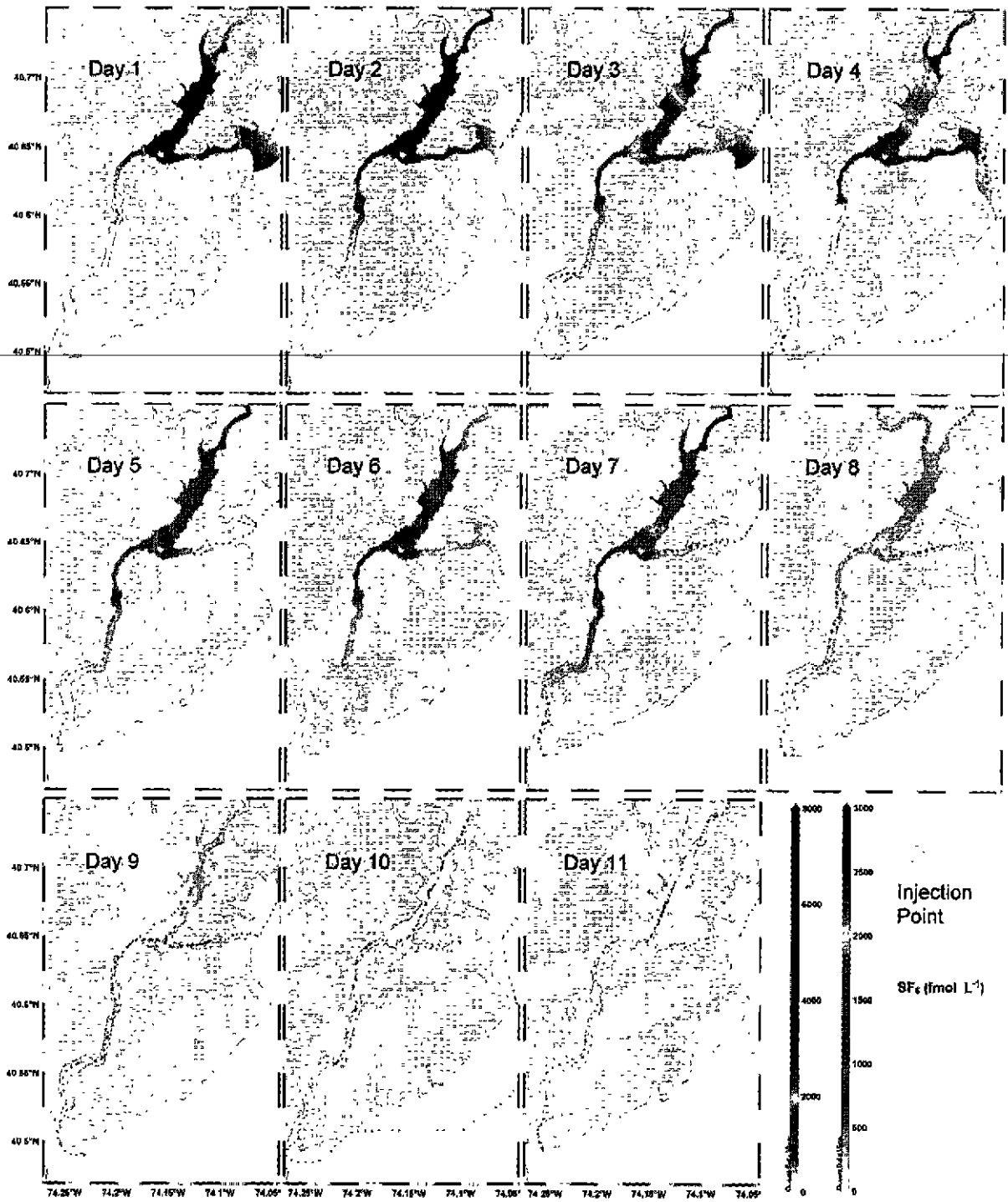

FIGURE 4. Complete series of daily average tracer measurements for 11 days, from July 15 (day 1) through July 25, 2002 (day 11). SF_6 was injected into NB on day 0.

the injection point and points inland (upriver), SF_6 concentrations were generally higher in bottom waters, whereas seaward of the injection point (NB and the Kills, i.e., the great majority of the study area), this gradient was reversed, and SF_6 diminished with increasing depth. This pattern suggests the influence of a slow estuarine circulation, with saline, low-SF_6 bottom water intruding into NB through the KVK and displacing the lower part of the initial SF_6 patch inland.

Over time, the vertical tracer gradient in NB and the kills diminished (Figure 6), as tidal flushing spread the SF_6 patch more evenly over the study area and carried large fractions of tracer into the KVK (where CTD data indicates rapid vertical mixing; see Figure 3) and into the Upper Bay. As a result, SF_6 was mixed earlier, and in larger relative quantities, into the intruding bottom water. If the profiles from NB are viewed separately from those in the kills (Figure 6), the diminishing gradient is still evident, demonstrating that this phenomenon is not an artifact of sampling location.

The mean vertical SF_6 gradient for complete profiles was $c_s \times (-0.024 \pm 0.020)$ m^{-1}, where c_s is the surface SF_6

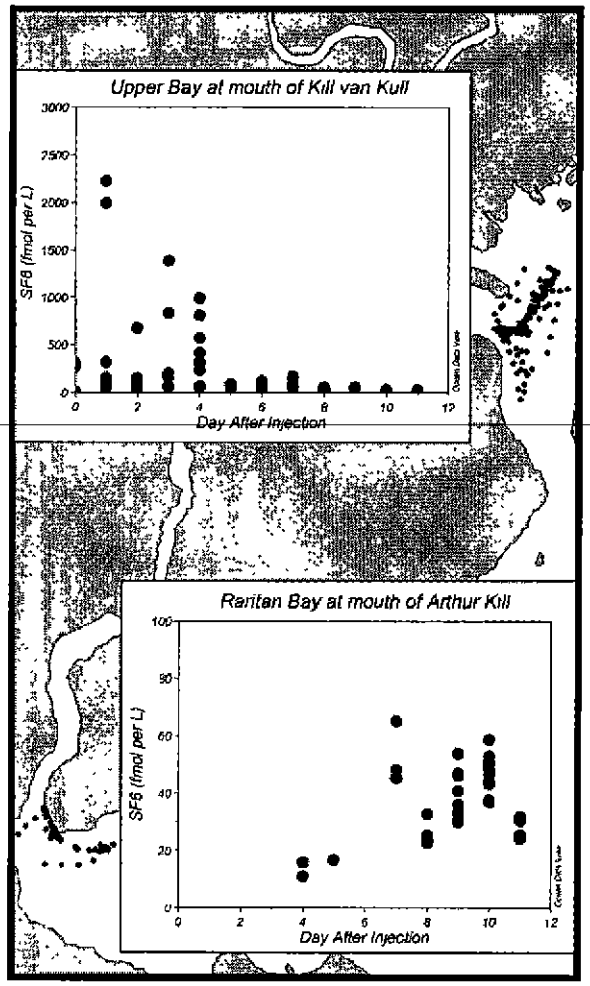

FIGURE 5. Comparison of all tracer measurements taken in regions lying immediately seaward of the KVK and the AK. Note the extreme difference in scale between the two regions. The KVK is revealed as the primary flushing pathway for Newark Bay, transporting tracer seaward much faster than the AK and at much higher concentrations. The concentration maximum at the mouth of the KVK occurs the day after injection, whereas the maximum at the mouth of the AK occurs a week after injection. (The large range in observations at the mouth of the KVK is due in part to variance in sampling location and tidal state between samples taken on the same day).

concentration (1 5 m depth). This gradient was multiplied by the average depth (10.0 m) and divided by 2 to determine a 0.12 ± 0.10 mean fractional excess of surface concentration above vertical mean concentration. The vertical profiles were neither sufficiently numerous nor sufficiently precise to warrant the use of a spatially or temporally distributed correction. Any error in the observed flushing rate caused by this approximation is small (of the order of 5%).

A combined mass inventory was calculated for the inner waterways (including the lower reaches of the Hackensack and Passaic rivers). The domain was divided into 18 reservoirs (boxes), and a wet volume for each reservoir was calculated on the basis of bathymetric data obtained from NOAA's Office of Coast Survey. The overall mean density of the bathymetry data was 62 measurements per box; near the latitudinal center of the study area, bathymetry resolution was ~100 m, declining to a resolution of ~400 m at the northern and southern extremes The mean SF_6 tracer concentration in each box was found for each day (mean data density: 10 measurements per box), the mean SF_6 depth profile (−0.024

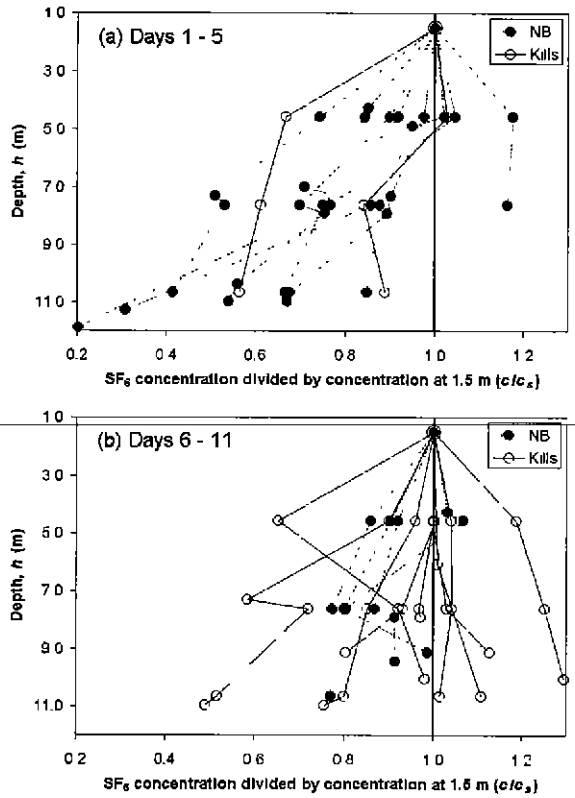

FIGURE 6. Vertical profiles of SF_6 from the first (a) and second (b) halves of the study period. All profiles recorded at or seaward of the injection point are displayed (one outlier was removed). The strong gradients in the earlier figure (a) suggest shearing of the tracer patch by estuarine circulation. The diminished gradients in both the kills (AK and KVK) and NB evident in the second half of the experiment (b) are consistent with lateral spreading of the tracer, creating more opportunities for mixing with the incoming bottom water.

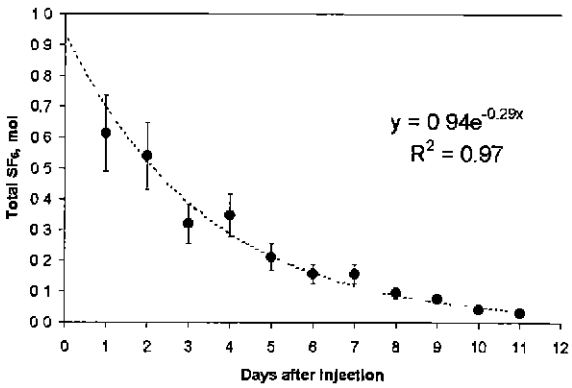

FIGURE 7. Total measured SF_6 inventory in the inner waterways over 11 days, with fitted exponential decay curve, indicating a decay constant (λ) of 0.29 ± 0.03 d^{-1} (this error is calculated from the variation of the points about the curve shown). Error bars (±20%) estimate the nonsystematic error at each point, caused primarily by daily averaging of samples taken at different times and along different paths.

c_s m^{-1}) was used to correct for depth gradients in the concentration, and the SF_6 in all of the boxes was added up to yield total SF_6 mass in the inner waterways. The resulting inventory (Figure 7) indicates that by day 7 (the time when the first significant concentrations of SF_6 began to emerge from the AK) the total SF_6 in the inner waterways had

decreased to 0.26 ± 0.06 times the amount measured on day 1. By day 10, this total had further decreased, to 0.07 ± 0.02 times the amount measured on day 1. The following exponential decay curve provides a good fit ($R^2 = 0.97$) to the full data set (11 days),

$$I_t = I_0\, e^{-\lambda t} \qquad (1)$$

where I_t is the inventory at time t, and t is the time that has passed since injection of the tracer, in days. I_0 and λ were determined to be 0.94 ± 0 18 mol and 0.29 ± 0.03 d^{-1} (mean residence time: 3 4 ± 0.4 days), respectively. This loss of tracer is the sum of air−water gas exchange and net flushing from the inner waterways to the Upper Bay (and to a lesser extent, to Raritan Bay). In a general sense, either of these processes, acting independently, should manifest itself as an exponential decay in tracer mass (neglecting the effects of fluctuations in wind speed and sea state on gas exchange, and neglecting the effects of fluctuations in tidal strength and river flow on flushing). Thus, it is not surprising that their sum is well represented by an exponential curve. The nonmonotonic behavior of SF_6 concentration at certain locations in Figures 4 and 5 and the consequent scatter in Figure 7 is assumed to be primarily due to differing states of the tide encountered during sampling transects on different days, with some additional contribution from varying sampling sequences through the main water bodies of the inner waterways (AK, KVK, NB).

Background Concentrations of SF_6. The mean SF_6 mixing ratio in the remote northern hemisphere atmosphere is ~5.0 ppt (February 2002, NOAA/CMDL), but studies have shown elevated levels in the New York metropolitan area, with a mean excess of 90% above the remote atmosphere in 1998−1999 measured at Palisades, NY, about 25 km north of New York City (*17, 18*). The Ostwald solubility coefficient for SF_6 is ~4.9×10^{-3} at 25 C, 1 bar, and a salinity of 20 (*19*). Thus, the expected concentration of SF_6 in New York Harbor at solubility equilibrium with the urban atmosphere is ~2 fmol L^{-1}.

Two SF_6 sampling surveys of the inner waterways, Upper Bay, and Hudson River were conducted in November and December 2002. Samples from a depth of ~1 m were pumped into 2-L glass bottles, and after flushing with several volumes, the bottles were capped without headspace. Laboratory analysis was performed on a GC-ECD system designed to measure SF_6 at environmental concentrations (*20*). Results from both surveys show SF_6 concentrations of 10−20 fmol L^{-1} in the inner waterways. Before injection on day 0 of the current study, the SF_6 concentrations in the study area were between 5 and 20 fmol L^{-1}. These levels are in excess of equilibrium concentrations due to unidentified sources. However, this SF_6 background did not limit the experiment in the inner waterways, where SF_6 concentrations remained above 40 fmol L^{-1} during the entire study period, and above 200 fmol L^{-1} until day 9. Outside the inner waterways, the SF_6 signal declined to background levels before the end of the experiment. A survey of the lower 18 km of the Hudson River on day 6 failed to detect SF_6 concentrations high enough to be attributed to the recent NB injection.

Discussion

No significant seaward advection of the peak SF_6 values is evident in the aggregate daily data sets (Figures 4 and 8). Seaward mixing of the tracer is attributed almost entirely to tidal action. Adding 7% to the Passaic River flow during the study period to account for the Hackensack River (ratio based on historical data) yields a combined freshwater flow from both rivers of 4.5 $m^3\, s^{-1}$. Dividing by the typical cross section of NB and the KVK (7500 m^2) yields an expected net advection of 52 m d^{-1}, an order of magnitude smaller than the probable residual circulation (Figure 2) and a displacement too small to detect given the larger flows in the system. By contrast, if the river flows were near the higher end of their typical annual range, the seaward movement would be of a size comparable to the residual circulation. For example, if flow on the Passaic River were in the 75th percentile of the 104-y record, the expected combined flow would be 50.3 $m^3\, s^{-1}$, and the expected net advection would be 580 m d^{-1} (4 km $week^{-1}$). In the case of a solute introduced into the surface layer, increased water column stratification under conditions of heavy runoff could lead to a two-layer flow, further accelerating net solute advection.

Despite the strong seaward movement of tracer through the KVK, the results do not preclude the slow counterclockwise residual circulation suggested by ADCP data and numerical flow modeling (*1, 2, 3*). It appears that a counter flow did not prevent the KVK from acting as the primary flushing pathway for solutes in NB, because of certain characteristics that allow this particular tidal strait to act as a unidirectional solute pump, repeatedly transferring solute from NB to the Upper Bay. (As with any tidal strait, the movement of water is bidirectional, but the transport of solutes is strongly biased in the seaward direction.) This tidal transfer dominates both adverse residual circulation and variations in freshwater flow and appears to depend on four characteristics: (a) strong tidal currents (peaking at ~1 m s^{-1} in the KVK); (b) a tidal strait comparable in length to, or shorter than, the mean tidal excursion (a 7-km strait vs a 13.4-km mean tidal excursion for the KVK); (c) a relatively confined body of water and related weak dilution at one end of the strait (the inland end of the KVK); and (d) a relatively open body of water and related strong dilution at the other end of the strait (the seaward end of the KVK). With these characteristics in place, the tidal strait becomes a powerful carrier of solutes toward the body of stronger dilution. This assertion must be tested by examination of other systems sharing the necessary characteristics.

The action of the KVK is further illustrated by examining a longitudinal section of SF_6 surface concentrations and surface salinity in the AK and NB on day 1 (Figure 8) A local minimum in the SF_6 concentration is juxtaposed with a local maximum in salinity at a point ~24 km along the section. This area marks the entrance of water from the KVK into NB. The intruding water is both saltier and lower in SF_6 as a result of enhanced mixing with the ocean water in the Upper Bay. The presence of this water in NB suggests that the tide was at late-stage flood at the time of this survey, and field notes confirm this inference, indicating slack before ebb (SBE) at 12:30, 10 minutes after the passage of the boat through this area. A similar pattern can be observed on days 2, 5, and 7 (Figure 8). In all of these cases, the tide was in late-stage flood as the boat arrived at the KVK/NB junction. Arrival times on the 3 days were 13.02, 14:42, and 16·33, corresponding to approximate SBE of 13:30, 16:30, and 18:30, respectively (field observations). On days 9, 10, and 11, the boat passed this point on the ebb tide, and the intrusion feature was either very small or did not appear (neither salinity nor SF_6 displayed significant local maxima or minima at the junction of the KVK and NB.) On days 3, 4, 6, and 8, the boat took a different route, and comparable transects were not obtained.

Air−Water Gas Transfer. Following Ledwell (*21*), in the presence of a vertical gradient in tracer concentration, the gas transfer velocity, k, can be calculated as

$$k = \frac{F}{(c_s - \alpha c_a)} = \lambda_g h \frac{\bar{c}}{c_s} \qquad (2)$$

where F is the mass flux across the air−water interface; c_a and c_s are the concentrations of gas in the air and in the

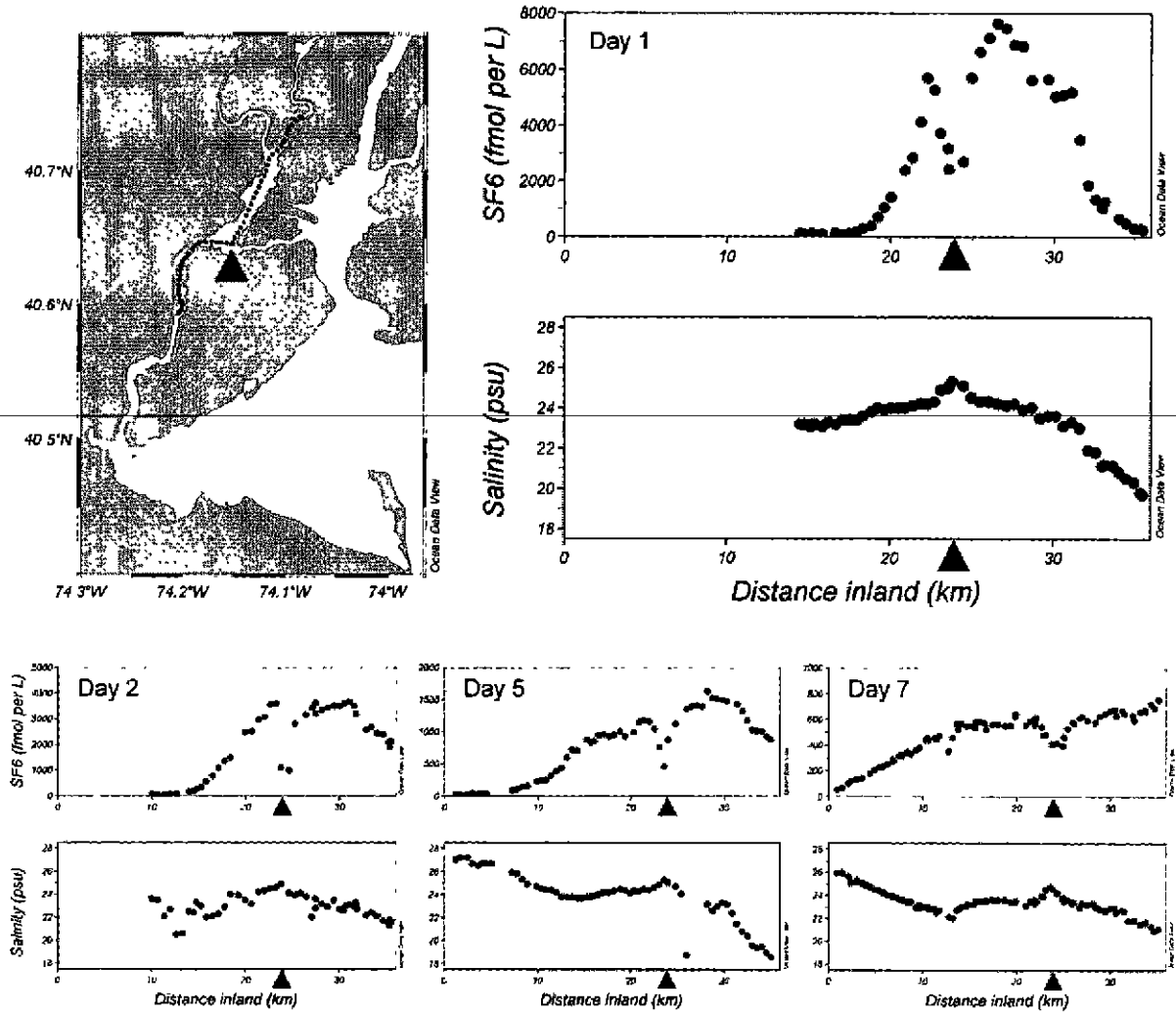

FIGURE 8. Longitudinal section of SF_6 concentration and salinity in the AK and NB on day 1 (July 15, 2002) and similar sections for days 2, 5, and 7 (July 16, 19, and 21, 2002). The map shows sampling locations for day 1; in subsequent days, sampling extended further down the AK. Distance inland is measured from the mouth of the AK.

water, directly above and below the air–water interface, respectively; $\bar{c}$ is the vertical mean concentration of the gas in the water; α is the Ostwald solubility coefficient for the gas in water; λ_g is the first-order gas transfer loss rate for the water column; and h is the mean water depth. For $\lambda_g \ll 1$, this equation is fairly insensitive to the distribution of depth across the study area. The last term on the right-hand side of eq 2 corrects for the observed mean excess of surface tracer concentration above the vertical mean tracer concentration ($c_s/\bar{c} = 1.12 \pm 0.10$).

Gas transfer velocities were estimated using two quadratic relationships between k and U_{10} (wind speed at 10 m height) that bracket a range of field data

$$k(600) = 0.222(U_{10})^2 + 0.333U_{10} \quad (3)$$

$$k(600) = 0.296(U_{10})^2 \quad (4)$$

where $k(600)$ is the gas transfer velocity normalized to a Schmidt number, Sc, of 600, corresponding to CO_2 in freshwater at 20 C (Sc = kinematic viscosity of water divided by molecular diffusivity of the gas in water). Equation 3 is from Nightingale et al. (*22*), and eq 4 is adapted from Wanninkhof (*23*). Clark et al. (*24*) demonstrate that k is correlated with U_{10} in the Hudson Estuary, and their results appear generally consistent with the relationships used here. (For streams and rivers, k is sometimes estimated via parametrizations based on flow velocities, an approach not pursued here because of large uncertainties in the temporal and spatial variation of flow velocities and also because wind is most likely the dominant source of near-surface turbulence in the study area). Wind data was obtained from a National Weather Service station at Newark Airport, ~5 km from the injection site across level terrain. Hourly wind speeds were applied to eqs 3 and 4 to determine a net $k(600)$ for each day of the study. From the mean conditions in the inner waterways (24.9 C, salinity = 24), Sc for SF_6 was determined to be 772 (*25*), and k for SF_6 was calculated from $k(600)$ by assuming that k was proportional to $Sc^{-0.5}$ (*26*). Equations 3 and 4 agreed to within 6% or better for all days except one (day 9), when the agreement was within 10%. Results were averaged over both equations, and all 11 days to yield a net $k(600)$ of 7.0 ± 0.4 cm h^{-1}, which in turn yielded a net λ_g of 0.17 ± 0.01 d^{-1}. This result represents the expected loss rate of SF_6 from the inner waterways if gas exchange were acting alone, that is, without flushing.

Flushing Rate. The loss of SF_6 from the inner waterways via gas exchange, predicted from wind speed, was plotted versus time (Figure 9). Total SF_6 losses from the inner waterways (eq 1) are shown on the same plot; the difference

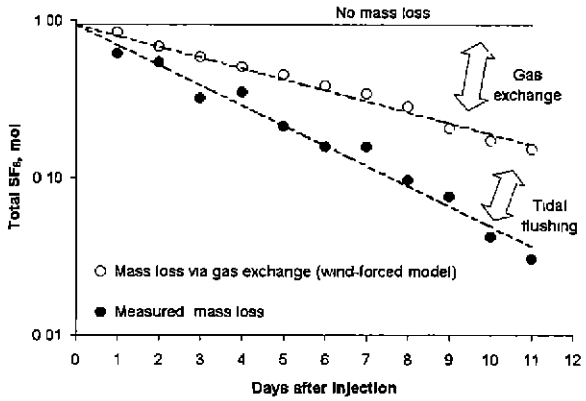

FIGURE 9. Modeled gas exchange mass loss and measured total mass loss in the inner waterways on a logarithmic scale. Tidal flushing accounts for the difference between the two loss rates. Both fitted lines have been forced to the same intercept at 0.94 mol.

between the two data sets represents the net flushing rate of the inner waterways,

$$\lambda_f = \lambda - \lambda_g \quad (5)$$

where λ_f is the first-order decay constant for flushing. The value of λ_f was determined to be $0.13 \pm 0.02\ d^{-1}$, representing the expected loss rate of SF_6 from the inner waterways if flushing were acting alone, that is, without gas exchange. The mean residence time in such a case would be 7.7 ± 1.4 days, as compared with the value of 3.4 ± 0.4 days observed for SF_6. If freshwater flushing were acting alone (i.e., no tidal flushing), residence time during the study period would have been of the order of 300 days. Under the high freshwater flow conditions described above (75th percentile), this result would be shortened to ~30 days. Similarly, if the counterclockwise residual circulation were acting alone, at a mean channel velocity of 1 cm s^{-1}, residence time would be of the order of 25 days. Thus, with the exception of gas exchange, tidal transfer in the KVK is by far the fastest process affecting solutes in the inner waterways.

For solute molecules at concentrations far above atmospheric equilibrium and with *Sc* in the same general range as SF_6, gas exchange is also a fast process, comparable to tidal transfer. Comparing λ_f and λ_g, gas exchange accounted for 56% of the loss of SF_6 from the inner waterways.

Tracer Transport in the AK. Significant levels of SF_6 were not detected at the seaward end of the AK until day 7 (Figure 4), indicating that tidal transfer was much less effective in this strait, as compared to the KVK, apparently because of its greater length and slower currents. (Additional significant differences may exist in the mixing behavior of Raritan Bay and Upper Bay) Residual circulation and longitudinal mixing appear to be the primary transport mechanisms for solutes and contaminants in the part of the AK that is far enough away from NB to be out of range of the KVK "pump" (roughly the lower two-thirds). Although complex interactions at both the seaward and inland ends of the AK make separate quantification of these mechanisms difficult, the net rate of tracer signal propagation in the AK can be characterized as follows:

A threshold concentration was chosen, defined as $1/e$ times the concentration at the most seaward peak. (Initially, transects through AK and NB contained only a single peak, but after the first few days, the tidal transfer of solute through

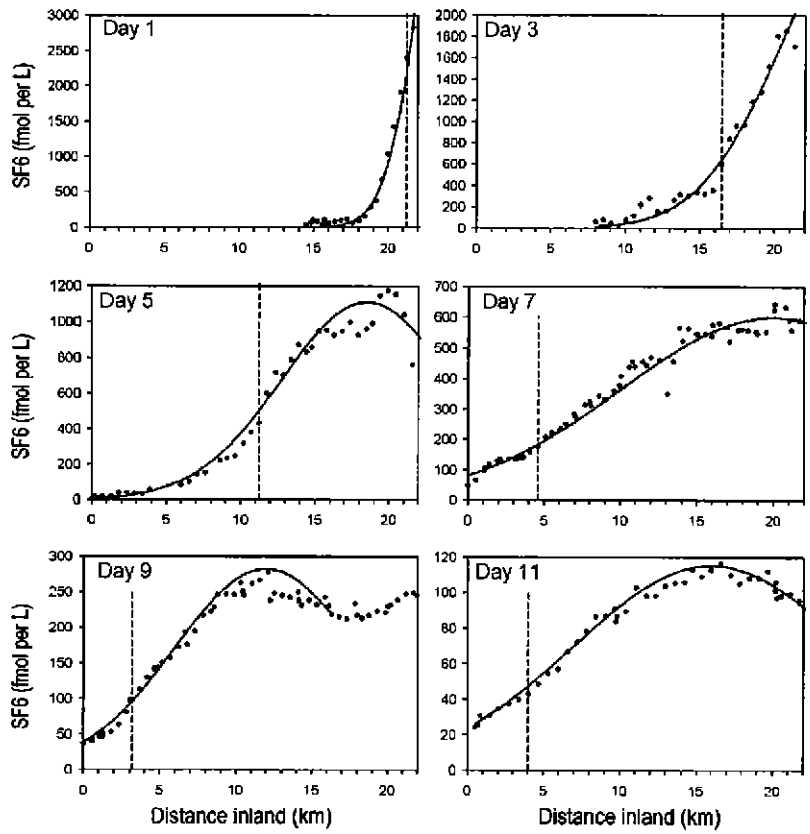

FIGURE 10. Progression of the SF_6 front seaward through the AK for representative days. The unbroken lines are Gaussian curves fit to the most seaward peak in the measured tracer data. The broken lines indicate the location of the "threshold" concentration, equal to $1/e$ of the peak concentrations. No tidal correction has been applied to this figure.

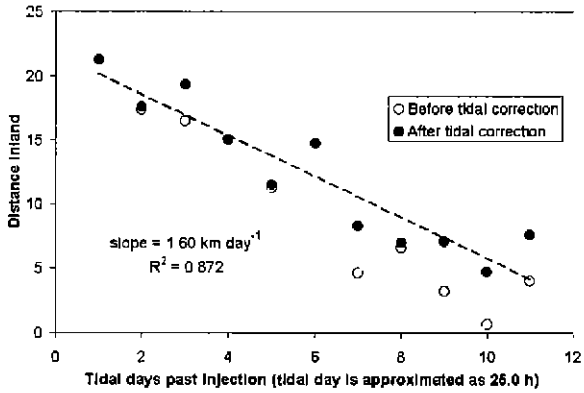

FIGURE 11. Position of the threshold SF_6 tracer concentration in the AK vs time. The threshold concentration, illustrated in Figure 10, is defined as 1/e of the concentration of the most seaward peak (see text). The location of the threshold concentrations were corrected to a common tidal state (slack before ebb) using a simple sinusoidal model calibrated to field observations. The open circles indicate the raw data without tidal correction. The threshold SF_6 signal moved down the AK at ~1.6 km d^{-1}.

the KVK created a local minimum at the northern end of the AK, as seen in Figure 8). Gaussian curves were fitted to the most seaward peak in the observed SF_6 distribution, the locations of the threshold concentrations were determined for days 1 to 11, and a selection of representative days was plotted (Figure 10). On each day, the threshold concentration defines the limit (in the AK) of the "bulk" of the tracer. This limit could have various applications, for example, a guideline for containment of a spill in Newark Bay, a delimiter for toxicological impacts, a quantitative measure for validation of numerical models, a normalized metric for comparison with other water bodies, etc.

A very simple tidal correction model was applied to relocate the threshold concentrations to their expected positions at the same state of the tide each day. Field observations indicated slack-before-ebb (SBE) conditions at the north end of the AK at 12:30 on day 1, and this time was assumed to advance 25 h each day. The locations of threshold concentrations were corrected to this time datum by assuming a sinusoidal tidal velocity with a maximum absolute velocity (in either direction, based on field observations) of 2 km h^{-1}. The location of the threshold concentration was plotted versus time for both the corrected and uncorrected data (Figure 11), revealing that the correction had a minor impact on the general result. The threshold concentration, as defined above, moved seaward through the AK at 1.60 ± 0.47 km d^{-1}. Comparison with the residual seaward circulation estimated from model data (~1 km d^{-1}) suggests that longitudinal dispersion is the cause of a significant fraction of the seaward transport.

Outlook. This experiment was one of the first to monitor tracer mixing, transport, and removal from a system of the size and complexity of the combined Newark Bay/Arthur Kill/Kill van Kull area. Future tracer work in this area would benefit from multiple injections in different locations or repeated injections in the same location, but subject to different forcing from tides, runoff, and wind. Experiments of this kind serve several purposes. Direct visualization is achieved of an accidental (or deliberate) contaminant release in a part of New York Harbor. The strength and nature of tidal estuarine mixing is explored, and certain results, in particular, the tidal transfer of solute through the KVK, might be applied to other water bodies. Finally, critical data for calibrating and validating hydrodynamic models of this region are obtained. Comparison with models is mutually beneficial, because once sufficiently validated, a model can explore a range of conditions at minimal cost, while helping to identify the most necessary empirical studies for future consideration.

Acknowledgments

We thank R. Enriquez for her contributions to the overall project, M. Garrison and H. Zahakos for assistance in the field, and B. Huber for assistance with the CTD. Special thanks to J. Lipscomb at Riverkeeper for expert handling of the research vessel; to E. Wei at NOAA's Office of Coast Survey for bathymetry and ADCP data, as well as flow modeling; and to M. Bruno, K. Rankin, and others at the Davidson Laboratory of Stevens Institute of Technology for advice and data on the study area. Three anonymous reviewers provided helpful comments. The Port Authority of NY and NJ provided trade and dredging statistics through the website <http://www.panynj.gov>. Streamflow and tide data were obtained from the USGS website <http://water.usgs.gov>, and Newark wind speed data was obtained from NOAA/NCDC. Information on the extent of local watersheds was obtained from The Environmental Statistics Group at Montana State University and from the NY–NJ Harbor Estuary Program. Remote SF_6 mixing ratios were obtained from NOAA/CMDL. Funding was provided by a generous gift from the Dibner Fund, by the Lamont Investment Fund, and the National Science Foundation through a Graduate Fellowship (T.C.). LDEO contribution no. 6526.

Literature Cited

(1) Chant, R. J. *J. Geophys. Res.* **2002**, *107*, C9, 3131
(2) Blumberg, A. F.; Khan, L. A.; St. John, J. P. *J. Hydraul. Eng.* **1999**, *125*, 799–816.
(3) Wei, E.; Chen, M. *Hydrodynamic Model Development for the Port of New York/New Jersey Water Level and Current Nowcast/Forecast Model System*; Technical Report NOS-OCS-12, National Oceanic and Atmospheric Administration, Office of Coast Survey; U.S. Department of Commerce. Silver Spring, MD, 2001
(4) Ledwell, J. R.; Watson, A. J., Law, C. S. *Nature* **1993**, *364*, 701–703.
(5) Maiss, M.; Ilmberger, J.; Zenger, A.; Münnich, K. O. *Aquat. Sci* **1994**, *56*, 307–328
(6) Clark, J. F.; Schlosser, P.; Stute, M.; Simpson, H. J. *Environ. Sci Technol* **1996**, *30*, 1527–1532.
(7) Ho, D. T.; Schlosser, P.; Caplow, T. *Environ. Sci., Technol.* **2002**, *36*, 3234–3241.
(8) Caplow, T., Schlosser, P., Ho, D. T. *J. Environ. Eng.*, submitted.
(9) Wanninkhof, R.; Ledwell, J. R.; Broecker, W. S. *J. Geophys. Res* **1987**, *92*, 14567–14580
(10) U.S. Environmental Protection Agency, Assessment and Modeling Division, Office of Mobile Sources *Commercial Marine Activity for Deep Sea Ports in the United States, Final Report*; Publication EPA420-R-99-020,U.S. Government Printing Office: Washington, DC, 1999
(11) Port Authority of New York and New Jersey, *Building a 21st Century Port*; Port Authority of New York and New Jersey New York, NY, 2000
(12) Crawford, D. W.; Bonnevie, N. L., Wenning, R. J. *Ecotox. Environ Safe.* **1995**, *30*, 85–100.
(13) Gunster, D. G.; Bonnevie, N. L.; Gillis, C. A.; Wenning, R. J. *Ecotox. Environ Saf* **1993**, *25*, 202–213.
(14) New York City Department of Environmental Protection *2001 New York Harbor Water Quality Report*; City of New York: New York, NY, 2002.
(15) U.S. Army Corps of Engineers, New York District. *Dredge Material Management Plan: Technical Appendix*; U.S. Government Printing Office: Washington, DC, 1999.
(16) Wei, E. National Oceanic and Atmospheric Administration, Office of Coast Survey; personal communication, 2003.
(17) Ho, D. T.; Schlosser, P. *Geophys. Res Lett.* **2000**, *27*, 1679–1682.
(18) Santella, N.; Ho, D. T.; Schlosser, P.; Stute M. *Environ. Sci Technol* **2003**, *37*, 1069–1074.
(19) Bullister, J. L.; Wisegarver, D. P.; Menzia, F. A. *Deep-Sea Res. I* **2002**, *49*, 175–187.
(20) Ho, D. T. Ph.D. Dissertation, Columbia University, 2001.
(21) Ledwell, J. R. Ph.D. Dissertation, Harvard University, 1982

(22) Nightingale, P. D.; Malin, G.; Law, C. S.; Watson, A. J.; Liss, P. S.; Liddicoat, M. I.; Boutin, J.; Upstill-Goddard, R. C. *Global Biogeochem. Cy.* **2000**, *14*, 373−387.
(23) Wanninkhof, R. *J. Geophys. Res.* **1992**, *97*, 7373−7382.
(24) Clark, J. F.; Wanninkhof, R.; Schlosser, P.; Simpson, H. J. *Tellus* **1994**, *46B*, 274−285.
(25) King, D. B., Saltzman, E. S. *J. Geophys. Res.* **1995**, *100*, 7083−7088
(26) Jähne, B., Munnich, K. O.; Bosinger, R.; Dutzi, A.; Huber, W., Libner, P. J. *J. Geophys. Res.* **1987**, *92*, 1937−1949.

Received for review March 5, 2003. Revised manuscript received August 6, 2003. Accepted August 20, 2003.

ES034198+